



Research Paper

Primary desmoplastic small round cell tumor of the tibia: PET/CT and MRI presentation of a rare case and review of the literature

Du Xuesong^{a,b}, Guo Hong^b, Zhang Weiguo^{b,*}

^a Department of Radiology, General Hospital of Central Theater Command of People's Liberation Army, Wuhan, China

^b Department of Radiology, Daping Hospital, Army Medical University, 10th Changjiang Road, Yuzhong District, Chongqing, China

ARTICLE INFO

Keywords:

Bone
PET/CT
MRI
Desmoplastic small round cell tumor
Prognosis

ABSTRACT

Desmoplastic small round cell tumor (DSRCT) was a soft tissue sarcoma of mesenchymal cell origin that typically exhibited a multi-phenotypic pattern of immunohistochemical staining. DSRCT mainly presented in the abdomen sites and primary occurrence in bone was exceptional. In this study, we reported a new case of primary DSRCT of the tibia in a 33-year-old man who had intermittent pain in the left tibia. Radiographs showed transparent lesions in the left upper tibial. MRI revealed a lobular, lytic and ill-identified lesion with adjacent soft tissues swelling of the upper left tibia. CT confirmed notable destruction and wormlike osteolysis of the bone cortex. PET/CT showed a mass of high uptakes, indicating the malignance. He accepted surgical resection with followed multi-agent chemotherapy, containing vincristine, doxorubicin, ifosfamide and etoposide. Clinically and radiologically, the patient did not show any evidence of recurrence or metastasis at 30 months after surgical treatment. Primary osteogenic DSRCT was extremely rare and should be considered in differential diagnosis of bone tumors.

1. Introduction

Desmoplastic small round cell tumor (DSRCT) was an extremely rare malignant tumor that affected mainly adolescents and young adults, with a marked male predominance of 5 to 1. It was first described in 1989 by Gerald and Rosai [1] and was considered as a member of the small round blue cell tumor family, which included small-cell carcinoma, Ewing's sarcoma, neuroblastoma, lymphoma, etc. [2]. Histologically, DSRCT consisted of nests of small round cells of primitive appearance embedded in a desmoplastic stroma, and typically showed co-expression of epithelial, mesenchymal, and neuron-specific enolase (NSE) markers. Cytogenetic analysis has also shown a distinctive molecular alteration involving chromosomes 11p13 and 22q12 resulting in EWSR1-WT1 fusion in DSRCTs as a diagnostic biomarker [3]. The tumor typically arose from the abdominal and pelvic peritoneum, however, primary DSRCTs in sites such as pleura [4], kidneys [5], salivary glands [6] and central nervous system [7] have also been described. Although DSRCT may rarely metastasize to bone, primary occurrence in bone was exceptional. Therefore, we reported a rare case of primary osseous DSRCT and demonstrated the positron emission tomography/ computed tomography (PET/CT) and magnetic resonance imaging (MRI) characteristics combined with strict long-term follow-up.

2. Case presentation

A 33-year-old man presented to the arthrolimb surgery department with a 3-month history of intermittent pain in the left lower limb. He had been treated with anti-inflammatory and analgesic measures (loxoprofen sodium) in the local hospital before presentation. The physical examination showed a mass about 4cm*7 cm in size located at the medial part of the upper left tibia, with III⁺ hardness, obvious tenderness and no obvious range of motion. Past surgical and family histories were unremarkable.

Radiographs showed transparent lesions in the left upper tibial (Fig. 1). The lesion was lytic and ill-identified with a wide area of transition and overlying cortical thickening. A small amount of periosteal reaction the adjacent soft tissues swelling were also noted, paralleling the tibia shaft. Magnetic resonance imaging (MRI) revealed upper left tibia lesions measuring 6.9cm*1.9cm*2.0 cm with mixed high T1WI, low T2WI signal and slightly high signal in short time inversion recovery (STIR) sequence (Fig. 2). The lesion was lobular with clear boundary and the border between the lesion and the surrounding normal bone was also clear. Notable destruction could be found in the bone cortex, and sheet exudation could be seen in surrounding muscles and soft tissues. Computed tomography (CT) confirmed the mass and showed enlarged medullary cavity of the proximal tibia on the left side,

* Corresponding author.

E-mail address: wgzhang01@163.com (Z. Weiguo).

<https://doi.org/10.1016/j.jbo.2019.100272>

Received 24 November 2019; Received in revised form 1 December 2019; Accepted 2 December 2019

Available online 03 December 2019

2212-1374/ © 2019 The Authors. Published by Elsevier GmbH. This is an open access article under the CC BY-NC-ND license (<http://creativecommons.org/licenses/by-nc-nd/4.0/>).

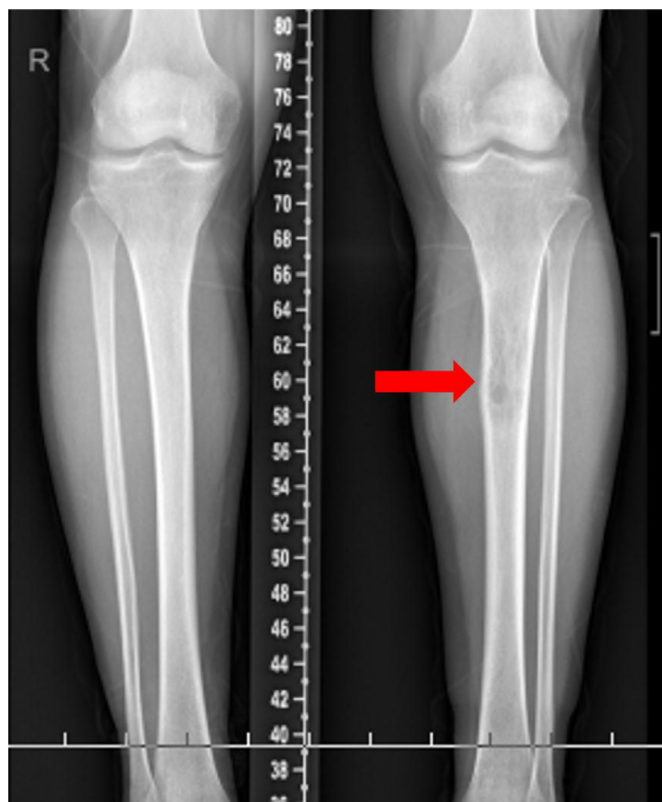


Fig. 1. Radiographs of the lesion. Low extremities radiographs showed transparent lesions in the left upper tibial. Periosteal reaction was present, as well as adjacent soft tissues swelling (red arrows).

and wormlike osteolysis of the cortex (Fig. 3). Poorly defined mineralization was also demonstrated. Positron emission computed tomography (PET) imaging showed a cluster of high uptakes of radioactivity (Fig. 4) with SUV_{max} of 24.66 and SUV_{avg} of 9.81 (standard uptake value, SUV). The leading radiological consideration was osteosarcoma, with other possibilities including Ewing's sarcoma and lymphoma. A CT scan of the chest, abdomen, and pelvis with intravenous contrast material revealed no lesions in other sites and whole-body PET scanning confirmed the lesion was consistent with a primary tibia mass.

The patient underwent surgical removal of the mass, with double plate internal fixation and bone cement packing. Part of the specimen was submitted for intraoperative consultation, and the frozen section was reported to be “malignant tumor of proximal left tibia”. Hematoxylin and eosin sections revealed a diffuse growth pattern replacing marrow space and eroding bone of the tumor. Tumor cells had a small amount of pale to clear cytoplasm, finely granular nuclei, and inconspicuous nucleoli (Fig. 4). Immunohistochemical staining revealed that the cells were strongly positive for CK, Desmin, CD99, Calretinin, CD56, P53, bcl-2, Fli-1 and WT-1 with Ki-67 index of 40% and negative for S100, Syn, CD34, SMA, Myogenin, MyoD1, CgA and TTE3. Molecular analysis identified an amplification of chimeric transcript corresponding to the EWS-WT1 gene rearrangement, indicating the presence of t(11;22)(p13: q12) reciprocal translocation. This result, along with the radiological, morphology and immunophenotype, declared the diagnosis for primary DSRCT in tibia.

The patient did well after surgery and was treated with multi-agent chemotherapy, containing vincristine, doxorubicin, ifosfamide and etoposide. He received regular follow-up every 3 months. Clinically and radiologically, the patient did not show any evidence of recurrence or metastasis at last follow-up, 18 months after surgical treatment.

3. Discussion

DSRCT was a member of the small round blue cell tumors family, which was consisted of distinctive neoplasms such as lymphoma, Ewing's sarcoma, Wilms tumor, neuroblastoma, etc. Distinct entities have been documented at an increasing number of anatomical sites, including central nervous system [8], kidney [5], testis [9], lung [10] and parotid gland [6]. Primary bone DSRCT was rare, to our knowledge, only 3 previous cases have been reported in the literature. This series was the first that reported the PET/CT imaging features of osseous DSRCT.

DSRCT was defined as a “malignant mesenchymal neoplasm composed of small round tumor cells with polyphenotypic differentiation embedded within a prominent desmoplastic stroma” in the recent WHO classification [11]. Histologic appearance was characterized by desmin, cytokeratin and S100, which were mesenchymal, epithelial and neural markers. Pathognomonic phenotype was identified as a unique t(11:22)(p13;q12) which resulted in an active fusion protein involving the Ewing sarcoma (EWS) and Wilms tumor (WT-1) genes [3,12]. DSRCT was reported more predominant in male patients, with a ratio of male to female of 4–5:1 [13,14]. The clinical symptoms were non-specific, and the disease most commonly presented as abdominal pain and distension, ascites and hydronephrosis, or symptoms related to rare extraperitoneal sites of the tumor.

Knowledge of the most common imaging features of DSRCT was important for guiding biopsy and appropriate patient management. It mainly presented as an intra-abdominal or pelvic mass with diffuse serosal involvement and peritoneal deposits in adolescent or young males [15]. DSRCT showed a higher rate of occurrence on serosal surfaces, where it appeared as single or multiple nodular masses on the surface of intra-abdominal organs. The characteristic imaging feature of DSRCT was multiple soft-tissue masses implicating the peritoneal cavity in the omentum or mesentery without a definite organ of origin as described in the literatures [16,17]. On CT images, tumor mass was usually patchy hypodense and mild heterogeneous enhancement on contrast enhanced images. DSRCT often appeared as lesions with isointense or hypointense on T1WI, hyperintense on T2WI, and heterogeneous enhancement on contrast-enhanced T1WI. Calcification was a relatively common radiological finding in abdominopelvic DSRCT [18].

DSRCT that primarily arose from bone was very rare. McDermott reported a case of desmoplastic small round cell tumor occurring in the right ilium of a 13-year-old boy in 2005, which was considered the first documented instance of desmoplastic small round cell tumor arising in bone [19]. CT and MRI scans of the pelvis showed a sclerotic bone lesion confined to the right ilium with no associated soft-tissue mass. In 2008, Panicek demonstrated a 10-year-old girl with primary DSRCT arising within the left femur [20]. Radiographs showed a large, predominantly lytic lesion in the distal femoral diaphysis with a wide zone of transition and overlying cortical destruction. Fritchie [21] retrieved 34 DSRCTs with atypical presentations and identified a 2.4-year-old male with located in the skull with no metastasis elsewhere. However, no investigations of image characteristics were found in the presentations.

In our study, we assess our experience with combined PET/CT and MRI for primary DSRCT in bone. Similar to morphology of DSRCT in other sites, primary bone DSRCT appears as solitary and lobular mass with a clear boundary. CT is most often used for initial diagnosis and follow-up, areas of low attenuation and non-enhancement are often present representing necrosis, hemorrhage or fibrous components. Punctate calcification can also be seen in this case and so as in previous two cases. MRI confirm this heterogeneity with mixed signal inside the lesion, for on T2W images, tumor mass shows a high signal “core” with a lower (but little higher than the muscle) signal “rim” around. The main tumor mass enlarges along the marrow cavity and causes a wide area of destruction and overlying cortical thickening. However, this perforating bone destruction is atypical on lower extremity

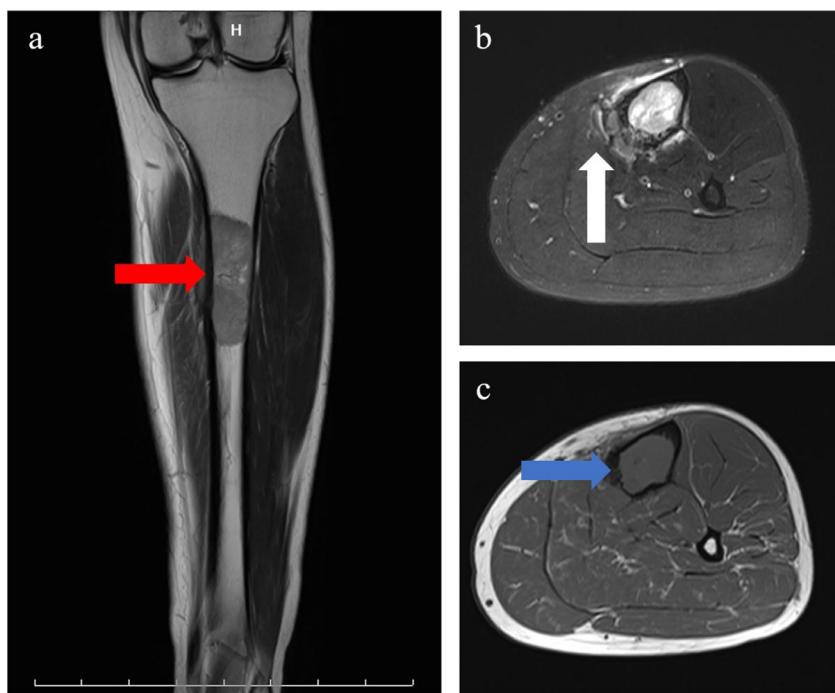


Fig. 2. Magnetic resonance imaging. a Coronal T1-weighted, b axial fat-saturated T2-weighted, and c axial T1-weighted. The lesion was lobular with clear boundary and the border between the lesion and the surrounding normal bone was also clear (red arrow). Notable destruction could be found in the bone cortex (white arrow), and sheet exudation could be seen in surrounding muscles and soft tissues (blue arrow).



Fig. 3. Computed tomography images confirmed the mass and showed enlarged medullary cavity of the proximal tibia on the left side, and wormlike osteolysis of the cortex. Poorly defined mineralization was also demonstrated.

radiographs; and thus, mimicking a benign behavior. As part of the staging evaluation principles, PET/CT is suggested for all patients with DSRCT [22]. However, this case is the first that reported the PET/CT imaging features of osseous DSRCT. The tumor mass appears with SUV_{max} of 24.66 and SUV_{avg} of 9.81, similar to the intra-abdominal masses [17,18], indicating that the mass is with high malignance.

The main differential diagnosis in this case was osteosarcoma, Ewing sarcoma and lymphoma. Osteosarcoma mainly occurred in young adolescent in the metaphysis of the longitudinal bone. Radiographs included various forms of bone destruction and tumor bone formation, different forms of periosteal neogenesis and destruction, soft tissue masses, bone destruction areas and tumor bone formation in soft tissue masses, etc. Ewing sarcoma mostly occurred in the diaphysis, extended from the center of the diaphysis to the metaphysis, and from the marrow cavity to the outside. Primary malignant lymphoma of bone was commonly seen in adult male patients. On radiographic images, the bone cortex can stay normal, and soft tissue mass with slightly high density can be seen in the marrow cavity. Ultimately, the presence of the EWS-WT1 fusion was the “gold standard” for the diagnosis of DSRCT [23].

Prognosis for DSRCT was quite poor, with five-year overall survival estimated at only 15 to 30% [24,25]. Primary osteogenic DSRCT was extremely rare, each of the reported patients presented in the bone was characterized by aggressive features, similar to DSRCT in other locations. In contrast, our case showed a very indolent clinical course.

In summary, primary osteogenic DSRCT was known as a rare subset of mesenchymal tumors. The radiologic features were of some specificity, but more confirmation was needed. Primary osteogenic DSRCT should be included in the differential diagnosis of bone tumors.

Funding

This work was supported by the Chongqing Science and Technology Commission (grant numbers: YDZX2017500004270).

CRediT authorship contribution statement

Du Xuesong: Conceptualization, Data curation, Writing - original draft. **Guo Hong:** Data curation. **Zhang Weiguo:** Writing - review & editing.

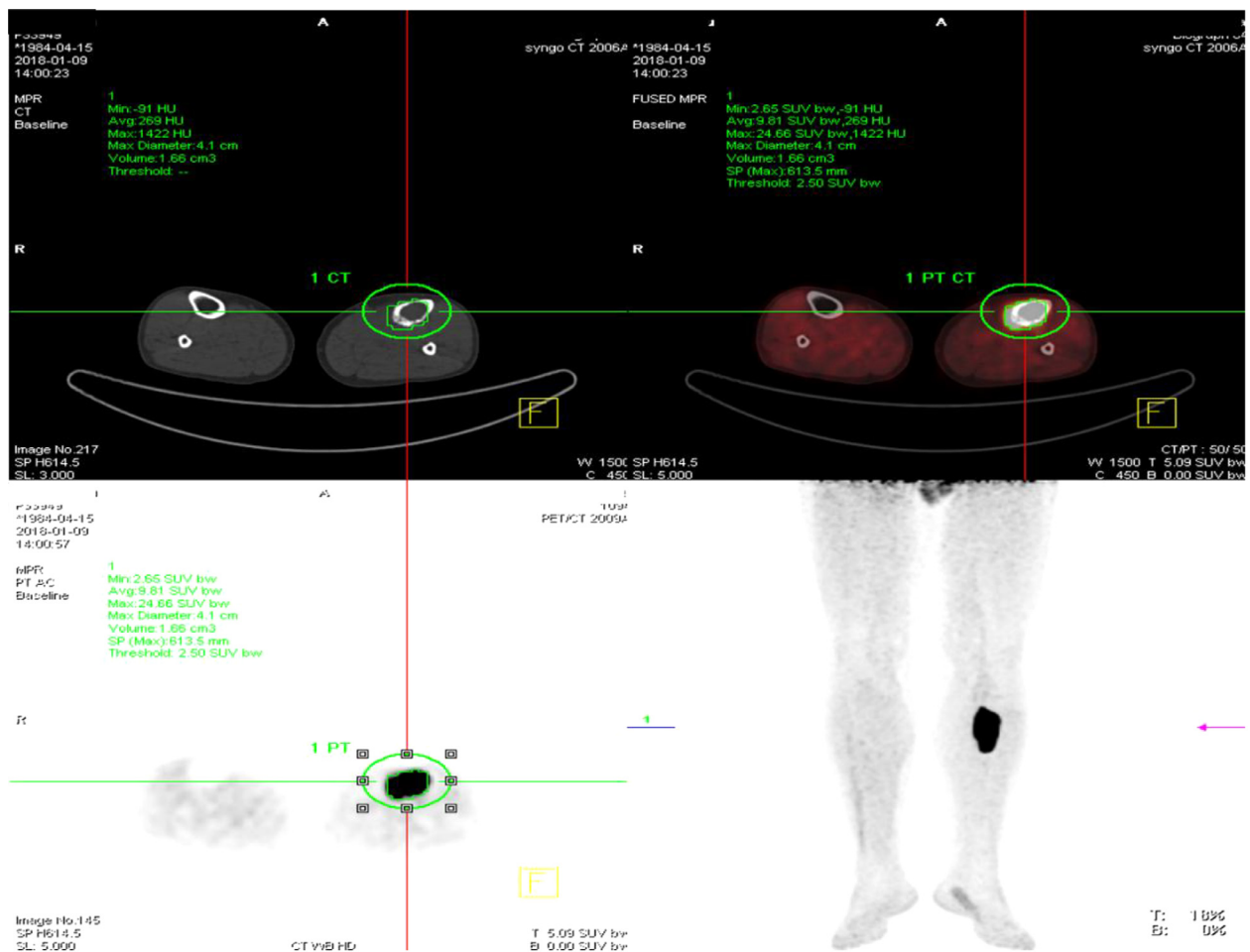


Fig. 4. Positron emission computed tomography imaging showed a cluster of high uptakes of radioactivity (Fig. 4) with SUVmax of 24.66 and SUVavg of 9.81 (green circle).

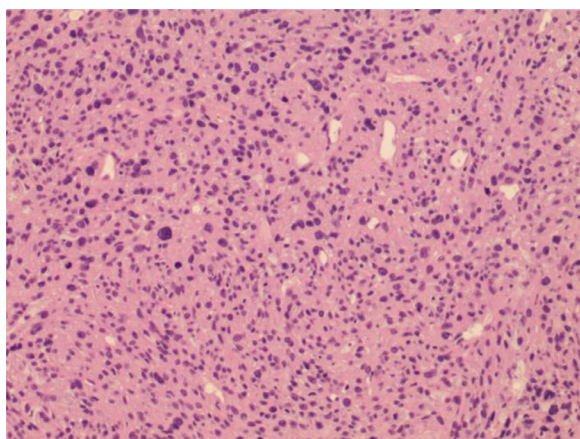


Fig. 5. Histopathologic findings sections revealed a diffuse growth pattern replacing marrow space and eroding bone of the tumor (Hematoxylin and eosin).

Declaration of Competing Interest

The authors declare that they have no conflict of interest.

Supplementary materials

Supplementary material associated with this article can be found, in

the online version, at [doi:10.1016/j.jbo.2019.100272](https://doi.org/10.1016/j.jbo.2019.100272).

References

- [1] W.L. Gerald, J. Rosai, Case 2. desmoplastic small cell tumor with divergent differentiation, *Pediatr. Pathol.* 9 (2) (1989) 177–183.
- [2] W.L. Gerald, H.K. Miller, H. Battifora, M. Miettinen, E.G. Silva, J. Rosai, Intra-abdominal desmoplastic small round-cell tumor. Report of 19 cases of a distinctive type of high-grade polyphenotypic malignancy affecting young individuals, *Am. J. Surg. Pathol.* 15 (6) (1991) 499–513.
- [3] M. Ladanyi, W.L. Gerald, Specificity of the EWS/WT1 gene fusion for desmoplastic small round cell tumour, *J. Pathol.* 180 (4) (1996) 462. doi:10.1002/(SICI)1096-9896(199612)180:4<462::AID-PATH694>3.0.CO;2-Y.
- [4] A.G. Fois, P. Pirina, A. Arcadu, F. Becciu, S. Manca, V. Marras, S. Canu, G. Castagna, G.C. Ginesu, A. Zinellu, P. Paliogiannis, Desmoplastic small round cell tumors of the pleura: a review of the clinical literature, *Multidiscip. Respir. Med.* 12 (2017) 22, <https://doi.org/10.1186/s40248-017-0103-6>.
- [5] M.J. Eklund, C. Cundiff, B.M. Shehata, A.L. Alazraki, Desmoplastic small round cell tumor of the kidney with unusual imaging features, *Clin. Imaging* 39 (5) (2015) 904–907, <https://doi.org/10.1016/j.clinimag.2015.05.002>.
- [6] K.C. Hatanaka, E. Takakuwa, Y. Hatanaka, A. Suzuki, I.I. S. N. Tsushima, T. Mitsuhashi, S. Sugita, A. Homma, S. Morinaga, T. Hashegawa, Y. Matsuno, Desmoplastic small round cell tumor of the parotid gland-report of a rare case and a review of the literature, *Diagn. Pathol.* 14 (1) (2019) 43, <https://doi.org/10.1186/s13000-019-0825-1>.
- [7] S.K. Thondam, D. du Plessis, D.J. Cuthbertson, K.S. Das, M. Javadpour, I.A. MacFarlane, J. Leggate, B. Haylock, C. Daousi, Intracranial desmoplastic small round cell tumor presenting as a suprasellar mass, *J. Neurosurg.* 122 (4) (2015) 773–777, <https://doi.org/10.3171/2014.10.JNS132490>.
- [8] L. Neder, B.W. Scheithauer, K.E. Turel, M.A. Arnesen, R.P. Ketterling, L. Jin, T.J. Moynihan, C. Giannini, F.B. Meyer, Desmoplastic small round cell tumor of the central nervous system: report of two cases and review of the literature, *Virchows. Arch.* 454 (4) (2009) 431–439, <https://doi.org/10.1007/s00428-009-0750-x>.
- [9] G.M. Zhang, Y. Zhu, H.L. Gan, D.W. Ye, Testicular desmoplastic small round cell

- tumor: a case report and review of literature, *World J. Surg. Oncol.* 12 (2014) 227, <https://doi.org/10.1186/1477-7819-12-227>.
- [10] M.A. Ariza-Protá, A. Pando-Sandoval, D. Fole-Vazquez, P. Casan, Desmoplastic small round cell tumor of the lung: a case report and literature review, *Respir. Med. Case Rep.* 16 (2015) 112–116, <https://doi.org/10.1016/j.rmcr.2015.08.010>.
- [11] I. Zambo, K. Vesely, [WHO classification of tumours of soft tissue and bone 2013: the main changes compared to the 3rd edition], *Cesk Patol.* 50 (2) (2014) 64–70.
- [12] B. Rekhí, R. Basak, S.B. Desai, N.A. Jambhekar, A t (11; 22) (p13; q12) EWS-WT 1 positive desmoplastic small round cell tumor of the maxilla: an unusual case indicating the role of molecular diagnosis in round cell sarcomas, *J. Postgrad. Med.* 56 (3) (2010) 201–205, <https://doi.org/10.4103/0022-3859.68628>.
- [13] R. Bellah, L. Suzuki-Bordalo, E. Brecher, J.P. Ginsberg, J. Maris, B.R. Pawel, Desmoplastic small round cell tumor in the abdomen and pelvis: report of CT findings in 11 affected children and young adults, *AJR Am. J. Roentgenol.* 184 (6) (2005) 1910–1914, <https://doi.org/10.2214/ajr.184.6.01841910>.
- [14] U. Tateishi, T. Hasegawa, M. Kusumoto, T. Oyama, H. Ishikawa, N. Moriyama, Desmoplastic small round cell tumor: imaging findings associated with clinicopathologic features, *J. Comput. Assist. Tomogr.* 26 (4) (2002) 579–583, <https://doi.org/10.1097/00004728-200207000-00018>.
- [15] V.C. Arora, A.P. Price, S. Fleming, M.J. Sohn, H. Magnan, M.P. LaQuaglia, S. Abramson, Characteristic imaging features of desmoplastic small round cell tumour, *Pediatr. Radiol.* 43 (1) (2013) 93–102, <https://doi.org/10.1007/s00247-012-2485-0>.
- [16] A.C. Morani, T.K. Bathala, V.R. Surabhi, S. Yedururi, C.T. Jensen, W.W. Huh, S. Prasad, A. Hayes-Jordan, Desmoplastic small round cell tumor: imaging pattern of disease at presentation, *AJR Am. J. Roentgenol.* 212 (3) (2019) W45–W54, <https://doi.org/10.2214/AJR.18.20179>.
- [17] J. Chen, Z. Wu, B. Sun, D. Li, Z. Wang, F. Liu, H. Hua, Intra-abdominal desmoplastic small round cell tumors: CT and FDG-PET/CT findings with histopathological association, *Oncol. Lett.* 11 (5) (2016) 3298–3302, <https://doi.org/10.3892/ol.2016.4421>.
- [18] W.D. Zhang, C.X. Li, Q.Y. Liu, Y.Y. Hu, Y. Cao, J.H. Huang, CT, MRI, and FDG-PET/CT imaging findings of abdominopelvic desmoplastic small round cell tumors: correlation with histopathologic findings, *Eur. J. Radiol.* 80 (2) (2011) 269–273, <https://doi.org/10.1016/j.ejrad.2010.06.046>.
- [19] A. Murphy, R.L. Stallings, J. Howard, M. O'Sullivan, R. Hayes, F. Breatnach, M.B. McDermott, Primary desmoplastic small round cell tumor of bone: report of a case with cytogenetic confirmation, *Cancer Genet. Cytogenet.* 156 (2) (2005) 167–171, <https://doi.org/10.1016/j.cancergencyto.2004.05.003>.
- [20] A. Yoshida, M.A. Edgar, J. Garcia, P.A. Meyers, C.D. Morris, D.M. Panicek, Primary desmoplastic small round cell tumor of the femur, *Skeletal. Radiol.* 37 (9) (2008) 857–862, <https://doi.org/10.1007/s00256-008-0501-0>.
- [21] A. Al-Ibraheemi, C. Broehm, M.R. Tanas, A.E. Horvai, B.P. Rubin, A.L. Cheah, K. Thway, C. Fisher, A. Bahrami, A.L. Folpe, K.J. Fritchie, Desmoplastic small round cell tumors with atypical presentations: a report of 34 cases, *Int. J. Surg. Pathol.* 27 (3) (2019) 236–243, <https://doi.org/10.1177/1066896918817140>.
- [22] A. Hayes-Jordan, H. Green, N. Fitzgerald, L. Xiao, P. Anderson, Novel treatment for desmoplastic small round cell tumor: hyperthermic intraperitoneal perfusion, *J. Pediatr. Surg.* 45 (5) (2010) 1000–1006, <https://doi.org/10.1016/j.jpedsurg.2010.02.034>.
- [23] V. Subbiah, S.E. Lamhamedi-Cherradi, B. Cuglievan, B.A. Menegaz, P. Camacho, W. Huh, V. Ramamoorthy, P.M. Anderson, R.E. Pollock, D.C. Lev, W. Qiao, M.F. McAleer, R.S. Benjamin, S. Patel, C.E. Herzog, N.C. Daw, B.W. Feig, A.J. Lazar, A. Hayes-Jordan, J.A. Ludwig, Multimodality treatment of desmoplastic small round cell tumor: chemotherapy and complete cytoreductive surgery improve patient survival, *Clin. Cancer Res.* 24 (19) (2018) 4865–4873, <https://doi.org/10.1158/1078-0432.CCR-18-0202>.
- [24] A. Dufresne, P. Cassier, L. Couraud, P. Marec-Berard, P. Meeus, L. Alberti, J.Y. Blay, Desmoplastic small round cell tumor: current management and recent findings, *Sarcoma* 2012 (2012) 714986, <https://doi.org/10.1155/2012/714986>.
- [25] C.K. Lettieri, P. Garcia-Filion, P. Hingorani, Incidence and outcomes of desmoplastic small round cell tumor: results from the surveillance, epidemiology, and end results database, *J. Cancer Epidemiol.* 2014 (2014) 680126, <https://doi.org/10.1155/2014/680126>.